Resveratrol improves skeletal muscle insulin resistance through downregulating lncRNA NONMMUT044897.2

Zhihong Liu
Hebei Medical University
Zhimei Zhang
Hebei Medical University
Guangyao Song (sguangyao2@163.com)
Hebei General Hospital https://orcid.org/0000-0002-9901-6074
Xing Wang
Hebei General Hospital
Hanying Xing
Hebei General Hospital
Chao Wang
Hebei General Hospital

Research

Keywords: High-throughput sequencing, Resveratrol, Long non-coding RNA, Insulin resistance

Posted Date: March 22nd, 2021

DOI: https://doi.org/10.21203/rs.3.rs-315719/v1

Abstract

Background: Long non-coding RNA (lncRNA) has proved to be crucial factors in the progression of insulin resistance (IR). Resveratrol (RSV) exhibits promising therapeutic potential for the IR. Nonetheless, whether RSV could influence the expression of lncRNAs and the interaction mechanisms in IR remain unclear.

Methods: We conducted high-throughput sequencing to detect the lncRNAs and mRNAs expression signatures and the co-expression network of lncRNAs and mRNAs in skeletal muscle after a high-fat diet (HFD)-induced IR mice model with or without RSV treatment, including hierarchical clustering, gene enrichment and gene co-expression networks analysis. Highly differentially expressed lncRNAs were selected and validated by RT-qPCR. Finally, the biological functions of the selected lncRNAs were investigated by silencing expressing the target genes through lentivirus transfection in C2C12 mouse myotubes cells.

Results: We revealed that 338 mRNAs and 629 lncRNAs whose expression in skeletal muscle after a high-fat diet (HFD)-induced IR mice model was reversed by RSV treatment. Gene Ontology and Kyoto encyclopedia of genes and genomes databases indicated that the differential expression mRNAs modulate the insulin signaling pathway. After validating randomly selected lncRNAs via RT-qPCR, we found that lncRNA (NONMMUT044897.2) and Suppressor of Cytokine Signaling 1 (SOCS1) were up-regulated in the HFD group, and reversed by RSV treatment. Additionally, NONMMUT044897.2 was validated to function as a ceRNA of microRNA (miR)-7051-5p and SOCS1 was confirmed as a target for miR-7051-5p. We further performed lentivirus transfection to knockdown NONMMUT044897.2 in vitro and found that NONMMUT044897.2 silence inactivated SOCS1 and promoted the insulin signaling pathway. Importantly, RSV could mimic the effects of silencing NONMMUT044897.2.

Conclusion: Our study revealed that resveratrol improves skeletal muscle IR might be via regulation of NONMUT044897.2.

1. Introduction

Insulin resistance (IR) has to be considered as a primary determinant for metabolic diseases, which reduce glucose uptake and utilization [1]. Skeletal muscle plays a significant part in the etiology of IR [2]. Resveratrol (3, 5, 4-trihydroxystilbene; RSV) is a kind of natural polyphenol, enriched in more than 70 kinds of plants [3]. Accumulating evidence has indicated that RSV displayed a diversity of biological activities [4, 5], including anti-oxidative, anti-aging, anti-inflammatory, hypoglycemic property, and attenuate insulin resistance [6, 7]. Several studies have indicated RSV possesses a satisfying anti-insulin resistance activity in skeletal muscle [8, 9, 10]. It is related to the activation of 5-adenosine monophosphate-activated protein kinase and restoration of glucose transporter 4 translocations [8, 9]. Our earlier research also proved that skeletal muscle insulin resistance caused by a high-fat diet may be alleviated after RSV treatment [10].

Long non-coding RNAs (lncRNAs) are a class of RNA molecules that more than 200 nucleotides in length and have little or no protein-coding capacity [11]. Growing research has shown that lncRNAs widely participate in plenty of developmental and physiological processes [12, 13], and are strongly correlated with the genesis and development of diseases, including coronary artery diseases [14], cancers [15], and metabolic diseases [16, 17]. Recently, the functions of lncRNAs in IR have gained a lot of attention [18, 19].

To date, however, there are limited studies on RSV regulating the function of lncRNAs. Given that, we intended to observe the effects and potential mechanisms of RSV on skeletal muscle IR of mice through measuring the whole genome expression profile of lncRNAs and mRNAs and to probe the correlation between RSV and lncRNA (NONMMUT044897.2) in improving IR in vivo and in vitro, providing new therapeutic targets for IR.

2. Materials And Methods

2.1. Animal experiments

We developed to control group, the high-fat (HFD) group, and the HFD + RSV group model by using C57BL/6J background mice (n = 14 in each group). Total 42 healthy 6 weeks old clean-grade C57BL/6J male mice weighing around 22g were purchased from Beijing Viton Lihua Experimental Center and sustained on a standard 12h light-dark cycles, with temperature (20–25°C) and humidity (40–60%). HFD mice were developed by feeding with a diet containing D12492J feed (20% protein, 20% carbohydrate, 60% fat) for 8 weeks. HFD + RSV mice were intragastrically applied with 100 mg/kg/day RSV solution for 6 weeks. Dissolved RSV (Sigma Aldrich, USA) with dimethyl sulfolane (Sigma Aldrich; 30 $mg.mL^{-1}$) and then diluted with 0.9%NaCl in a ratio of 1:2. For control mice, were received normal chow (D12450J contains 20% protein, 70% carbohydrate, and 10% fat). Weight and food intake were measured weekly during feeding. After the feeding experiment, all mice fasting for 12 hours and then were received intraperitoneal injection of 50% glucose (1.5g.kg-1 bodyweight) for glucose tolerance tests (IPGTT). Blood glucose was detected from the tail vein with a glucose meter at 0, 15, 30, 60, and 120 minutes post-injection, and the model of insulin resistance was validated by the area under the curve (AUC). Animal studies were approved by the ethics committee of the Hebei General

Hospital, and all animal experimental procedures complied with the National Institutes of Health guide for the care and use of laboratory animals.

2.2. Serum and tissue samples

Three mice in each group were randomly selected and given an intraperitoneal injection of 1.5U/40g of insulin (Sigma Aldrich). Cervical dislocation and euthanasia were performed 20 min later. The blood samples were gathered by puncture heart and then centrifuged at 3000×g at 4°C for 10min, then the serum was stored at -80℃. Collected skeletal muscles were withdrawn quickly and stored in liquid nitrogen for the follow-up study.

2.3. Serological indicators were tested

Detection kits for total cholesterol (TC), triglyceride (TG), high-density lipoprotein cholesterol (HDL-C), low-density lipoprotein cholesterol (LDL-C), and free fatty acid (FFA) were acquired from Nanjing JianCheng Institute of Biological Engineering (Jiangsu, China). Serum insulin was obtained with an ELISA kit (ALPCO Diagnostics, USA). All steps followed the manufacturer's protocol.

2.4. Western blot

The same amount of protein with different groups was separated by sodium dodecyl sulfate-polyacrylamide gel electrophoresis, then transferred to PVDF membrane and sealed with 5% skimmed milk for 2 h. Diluted the primary antibodies in the blocking solution at the following concentration:β-actin: rabbit antibody, 1:5000; GAPDH: rabbit antibody, 1:10000; AKT: Rabbit antibody, 1:1000;p-AKT(Ser 473): Rabbit antibody, 1:750; GSK3β: Rabbit antibody, 1:750; p-GSK3β: Rabbit antibody, 1:750; GLUT4: Rabbit antibody, 1:5000, SOCS1: Rabbit antibody, 1:5000. The antibodies were acquired from Cell Signaling Technology (Danvers, USA) and Abcam (Cambridge, UK). PVDF membranes and primary antibodies were incubated at 4℃ for 24h. Washed and incubated membranes with second antibodies at RT for about 50 minutes and then washed three times for 10 minutes each time. Protein bands were calculated by densitometry taking advantage of the Image J software and normalized to β-actin or GAPDH levels.

2.5. RT-qPCR

Total RNAs were extracted with Trizol reagent and then tested for RNA purity and concentration using NanoDrop 2000 (Fisher Scientific, USA). The PrimeScript™ RT Reagent Kit with gDNA Eraser was reverted and amplified with SYBR® Premix Ex Taq™ II Kit (RR820A). Applied Biosystems 7500 real-time PCR systems to perform RT-qPCR, with a total of 41 cycles, including 3 minutes of pre-denaturation at 95°C, 5 seconds at 95°C, and 32 seconds at 60°C. The melting point curve was established at 60–95°C. β-actin and U6 were considered as an internal reference control for genes, respectively. The relative gene expression was quantified by the $2^{-(\Delta\Delta Ct)}$ method [20]. The specific primers involved in this research are listed in Table 1.

Table 1
Real-time quantitative polymerase chain reaction primers used in this study

Gene	Forward primer (5'-3')	Reverse primer (5'-3')
β-actin	GGCGCTTTTGACTCAGGATT	GGGATGTTTGCTCCAACCAA
NONMMUT139818.1	TGGGTCCTTGGTGTTCTTGTT	TCTAAAGTGGAGCCAACAAAGG
NONMMUT044897.2	TCCCAAAGAGTTCCGAAGGTA	GTGATGACACCAGGTATGACGG
NONMMUT005295.2	AGGCTTGTCTGAGGTTGCTGG	TTTACATCCTTGGGCTGCTTT
NONMMUT071570.2	TCTCCTGGGCTTCCCTAACTAA	CTCCCAAGGGCAGCATAACA
NONMMUT065156.2	GTTGCCATTCATCCTACCTCTTC	ATCAAATGAAAACCAACCCCG
NONMMUT00000181045	CAGCCAAATCACCAACAAACAGA	CCCTTACTCATAAATCAGCCTCACC
NONMMUT128951.1	GCTGGTCAAGCCAACAAGTAGT	GGCACCACATTGAACAGTAAAGTC
NONMMUT145909.1	AAGGGTGGACCAAGGCTAAAC	ACTGGCATCCTCAAACCTCAA
AKT	AAGGAGGTCATCGTCGCCAA	ACAGCCCGAAGTCCGTTATC
GSK3β	AAGGACTCACCAGGAGCAGGA	ATGTGGAGGGATAAGGATGGTG
SOCS1	CCGTGACTACCTGAGTTCCTTC	ATGAGGTCTCCAGCCAGAAGTG
mmu-miR-7051-5p	CTCAACTGGTGTCGTGGAGTCGGCAATTCAGTTGAGTGACCCAA	ACACTCCAGCTGGGTCACCAGGAGGAAGTT
CTCGCTTCGGCAGCACA	AACGCTTCACGAATTTGCGT	

2.6. cDNA library construction and RNA sequencing.

LncRNAs and mRNAs were quantitative analysis by Sinotech Genomics Co., Ltd (Shanghai, China). Illumina Novaseq 6000 was used to construct a high-throughput RNA sequencing based on the removal of ribosomal RNA. Fastp software was performed to filter the sequence to get the clean reads. Clean reads were mapped to the GRCM38 reference genome using Hisat2. Each gene fragment was counted using Stringtie software contrast and then normalized by using the TMM (trimmed mean of M values) algorithm and then calculated FPKM value of each gene.

2.7. Differential expression of lncRNAs and mRNAs analysis.

The differential expression of skeletal muscle in three groups was analyzed based on the edgeR software package. The threshold of the p-value was confirmed by controlling the False Discovery Rate. The screening criteria for differential expression of mRNAs and lncRNAs were $P < 0.05$ and fold change (FC) > 2.0.

2.8. Functional group analysis.

Gene Ontology (GO) and Kyoto Encyclopedia of Genes and Genomes (KEGG) pathway were determined the potential role of the lncRNAs co-expressed with the differentially expressed mRNAs. GO analysis was implemented to establish significative annotations of genes and gene products in diversified organisms using the DAVID database (http://david.abcc.ncifcrf.gov). In addition, KEGG pathway analysis was used to make differential expression mRNAs in enriched pathways. $P < 0.05$ was identified as the significance threshold.

2.9. Co-expression network.

The co-expression network of NONMMUT044897.2 and microRNA and mRNA was analyzed by using Cytoscape software 3.6.0 (Cytoscape, USA).

2.10. C2C12 cell culture and treatments

C2C12 mouse myotubes cells were maintained in Dulbecco's modified Eagles medium (DMEM; Gibco, USA) containing 10% fetal bovine serum (San Diego, USA) and 1% penicillin/streptomycin (Wisent, China,) at 37 °C with 5% CO2. Cells differentiation was induced by incubation for 4 days in DMEM containing 2% FBS after reaching 80% confluence. Differentiated C2C12 cells were incubated for 24 hours with 0.25mM palmitate (PA)[21] (Aladdin Industries, China).At 0h, 8h, 16h, 24h after the intervention of PA, the glucose concentration in the culture medium was determined by the glucose oxidase assay to determine whether the insulin resistance model was established. Subcultured C2C12 cells were digested to prepare a cell suspension and then subcultured to a 96-well culture plate. When the cells grew to about 80%, add resveratrol medium with different concentrations of 100μM, 50μM, and 30μM. After 24 hours, add 10ul of CCK-8 to each well (need to be protected from light), culture for 20 minutes, measured the absorbance at 450 nm and calculated the cell survival rate. C2C12 cells in the logarithmic growth phase were subcultured in a 6-well plate and then transfected with lentivirus. Synthesized constructs including LV3-NC (5' to 3' TTCTCCGAACGTGTCACGT), LV3-NONMMUT044897.2 (5' to 3' GCTCTTTCAGATAAGCCTTGT) obtained from Genepharma Co., Ltd. China. Stable cell lines were obtained after puromycin selection for the PA-induced IR model and drug intervention experiments. The plated cells were grouped: control group (CON), PA group (PA), PA + shRNA-NONMMUT044897.2 negative control group (PA + shRNA-NC), PA + shRNA-NONMMUT044897.2 knockdown group (PA + shRNA-NONMMUT044897.2), and PA + RSV 30μM group (PA + RSV). After successful modeling, the glucose concentration was detected for 24 hours, and the NONMMUT044897.2 and miR7051-5p mRNA expression levels were measured by RT-qPCR. The cells were stimulated with insulin, and the protein was extracted 20 minutes after insulin stimulation for Western blot analysis and also cell cultures were extracted by TRIzol reagent (Invitrogen).

2.11. Statistical analysis

SPSS23.0 was used for data analysis and the results were indicated as mean ± SD. One-way ANOVA was performed for comparison between groups. $P < 0.05$ was defined as statistically significant.

3. Results

3.1. Establishment of IR animal model developed by a high-fat diet

Before the intervention, the body weight of the control group (CON) was similar to that of the high-fat diet group (HFD). After one week of dietary intervention, HFD mice were dramatically heavier than CON mice (Fig. 1A), while their average daily calorie intake was comparable (Fig. 1B). Besides, the intraperitoneal glucose tolerance test (IPGTT) 8 weeks after dietary intervention showed that the blood glucose level of the HFD group was drastically elevated compared with the CON group(Fig. 1C) at 0, 30, 60, and 120 minutes after glucose saline injection. Meanwhile, the HFD group resulted in a remarkable augment of AUC in contrast to the CON group, (Fig. 1D), indicating that the insulin resistance model was successfully established.

3.2. RSV ameliorates body weight,insulin resistance and lipid levels in HFD-fed mice

After 2 weeks of resveratrol (RSV) administration, the weight of the HFD + RSV group was greatly declined than that of the HFD group (Fig. 2A), although the daily calorie intake between the groups was similar(Fig. 2B). Also, RSV treatment restricted the blood glucose level of IPGTT and AUC level (Fig. 2C, 2D). As compared with the CON mice, fasting blood glucose was robustly elevated in the HFD group as well as insulin levels (Fig. 2E, 2F).RSV treatment showed a marked reduction in both of them(Fig. 2E, 2F). The quantitative insulin sensitivity index (QUICKI) of HFD mice was declined than that of CON and HFD + RSV groups (Fig. 2G). As compared with the CON group, the levels of TG, TC, LDL-C, and FFA were strikingly increased in the HFD group. Also, RSV treatment could abolish the up-regulation of TG, LDL-C, and FFA in the HFD group, while TC decreased but had no significance (Fig. 2H-L). There was no difference in high-density lipoprotein cholesterol (HDL-C) of the mice.

3.3. RSV treatment reduced SOCS1and increased phosphorylation of AKT and GSK3β in HFD mice

In the CON, HFD, and HFD + RSV mice, no differences were found in the mRNA and protein levels of AKT and GSK3β (Fig. 3A, 3B, 3D, 3E, 3G). The HFD group dramatically repressed p-AKT and p-GSK3β protein levels compared with the CON group, and the RSV treatment showed a marked increase in p-AKT and p-GSK3β protein expression (Fig. 3D, 3F, 3H). Moreover, Suppressor of Cytokine Signaling 1 (SOCS1) in the HFD group was abnormally elevated, and the increase in the expression of SOCS1 was abrogated upon RSV treatment (Fig. 3C, 3D, 3I). These results suggest that RSV improves gene expression on the insulin signaling pathway.

3.4. RSV systematically modulates skeletal muscle gene expression

The expressions of lncRNAs and mRNAs in CON, HFD, and HFD + RSV were determined by high-throughput sequencing. Results demonstrated that after standardization, 58245 lncRNAs and 83089 mRNAs were identified in the skeletal muscle of mice. By comparison of HFD with the CON group, there were 3276 differentially expressed lncRNAs (1192 up-regulated and 2084 down-regulated) and 2118 differentially expressed mRNAs (314 up-regulated and 1804 down-regulated). Simultaneously, there were 1640 differential expression lncRNAs (921 up-regulated and 719 down-regulated) and 604 differential expression mRNAs (444 up-regulated and 160 down-regulated) in the HFD + RSV group compared with the HFD group. Among the up-regulated lncRNAs and mRNAs in the HFD group, 270 lncRNAs and 58 mRNAs were down-regulated in the HFD + RSV group. Among the lncRNAs and mRNAs down-regulated in the HFD group, 359 lncRNAs and 280 mRNAs were up-regulated in the HFD + RSV group. The top 30 differential expression lncRNAs and mRNAs are listed in Table 2 and 3. With FPKM 0 were eliminated.

Table 2
Top 30 significantly differential expression lncRNAs in mice.

lncRNA_id	log2FC (HFDvsCON)	Pvalue (HFDvsCON)	Updown (HFDvsCON)	log2FC (HFD + RSVvs HFD)	Pvalue (HFD + RSVvs HFD)	Updown (HFD + RSVvs HFD)
NONMMUT147944.1	7.361654305	3.08E-05	UP	-7.65705	2.59E-05	DOWN
NONMMUT018494.2	6.726119826	2.72E-30	UP	-6.63171	1.25E-30	DOWN
NONMMUT056862.2	6.372532912	0.000101	UP	-6.47057	0.000104	DOWN
NONMMUT001029.2	5.951073546	1.73E-06	UP	-6.20954	1.09E-06	DOWN
NONMMUT034722.2	5.925450571	5.74E-05	UP	-5.99116	5.98E-05	DOWN
NONMMUT042491.2	5.439454581	0.000152	UP	-6.0331	6.81E-05	DOWN
NONMMUT011659.2	5.319133003	0.000118	UP	-5.39538	0.000122	DOWN
NONMMUT028972.2	5.109498067	9.40E-05	UP	-5.33988	7.69E-05	DOWN
NONMMUT056994.2	4.330643092	1.11E-07	UP	-3.97586	2.22E-06	DOWN
NONMMUT044528.2	4.3149951	2.45E-05	UP	-4.67614	1.12E-05	DOWN
NONMMUT139818.1	4.27510251	5.42E-10	UP	-2.93598	3.09E-07	DOWN
NONMMUT006490.2	4.040499067	4.37E-05	UP	-4.25073	3.25E-05	DOWN
NONMMUT153460.1	3.987910041	1.14E-10	UP	-4.43375	1.79E-11	DOWN
NONMMUT047957.2	3.622830463	5.31E-12	UP	-2.17202	1.80E-06	DOWN
NONMMUT061044.2	3.580172631	0.000913	UP	-5.02265	0.000116	DOWN
NONMMUT041793.2	3.348027654	0.000102	UP	-4.15666	2.47E-06	DOWN
MSTRG.26789.5	3.346146359	4.90E-17	UP	-2.35799	1.25E-05	DOWN
NONMMUT141647.1	3.045932847	2.40E-05	UP	-3.7519	3.30E-05	DOWN
NONMMUT019242.2	2.994018555	1.34E-16	UP	-1.86027	2.37E-07	DOWN
NONMMUT054892.2	2.304363454	8.76E-08	UP	-1.99848	3.44E-05	DOWN
NONMMUT051479.2	2.213054794	0.00098	UP	-3.05151	3.84E-05	DOWN
NONMMUT003238.2	2.187198497	0.045286	UP	-5.56027	8.43E-05	DOWN
NONMMUT004274.2	2.077962645	1.51E-05	UP	-1.86821	0.000128	DOWN
NONMMUT006717.2	2.041245592	1.41E-06	UP	-2.02194	8.66E-06	DOWN
ENSMUST00000145549	1.981088074	3.80E-07	UP	-1.97828	7.99E-07	DOWN
NONMMUT071342.2	1.630473739	0.012079	UP	-3.80688	1.60E-13	DOWN
NONMMUT005295.2	1.449638857	1.11E-06	UP	-1.41758	2.03E-05	DOWN
NONMMUT070926.2	1.34488241	0.026106	UP	-2.66561	8.38E-08	DOWN
NONMMUT006953.2	1.275954985	0.000623	UP	-2.36716	2.40E-09	DOWN
NONMMUT044897.2	1.249501171	2.60E-05	UP	-1.43116	2.19E-05	DOWN
NONMMUT048831.2	-1.272978476	0.046708	DOWN	1.547263	0.000408	UP
NONMMUT018620.2	-1.425732816	0.032203	DOWN	1.762165	0.000445	UP
NONMMUT051818.2	-1.49981749	0.00019	DOWN	1.757541	0.000229	UP
NONMMUT148959.1	-1.821849383	0.022286	DOWN	2.39635	0.000835	UP
NONMMUT025210.2	-1.865766716	0.032229	DOWN	3.501751	1.41E-09	UP

The table lists the top 30 of the results for lncRNAs with an up-or downregulation in expression in three groups.

lncRNA_id	log2FC (HFDvsCON)	Pvalue (HFDvsCON)	Updown (HFDvsCON)	log2FC (HFD + RSVvs HFD)	Pvalue (HFD + RSVvs HFD)	Updown (HFD + RSVvs HFD)
NONMMUT024340.2	-1.99805347	6.44E-07	DOWN	1.727535	0.000114	UP
NONMMUT030788.2	-2.072643561	0.008364	DOWN	3.386966	6.32E-08	UP
NONMMUT083064.1	-2.184391746	0.02567	DOWN	3.578567	9.44E-07	UP
NONMMUT117757.1	-2.220356685	0.000126	DOWN	1.946318	0.000268	UP
NONMMUT145026.1	-2.225432629	0.005502	DOWN	2.733938	0.00075	UP
NONMMUT143802.1	-2.239123899	0.000257	DOWN	2.484837	0.000105	UP
NONMMUT081465.1	-2.275670974	0.000759	DOWN	2.214893	0.000569	UP
NONMMUT071570.2	-2.342779878	1.52E-05	DOWN	2.040383	7.76E-05	UP
NONMMUT145721.1	-2.395813608	0.00904	DOWN	3.144452	0.000475	UP
NONMMUT082610.1	-2.721997741	0.004713	DOWN	3.500026	3.04E-06	UP
NONMMUT032162.2	-2.756781381	0.000975	DOWN	3.252807	1.74E-06	UP
NONMMUT098269.1	-2.860045031	2.20E-09	DOWN	2.306565	0.000783	UP
NONMMUT119847.1	-2.871001568	6.07E-06	DOWN	2.197726	0.000589	UP
NONMMUT004497.2	-3.006495667	6.12E-06	DOWN	3.18202	2.60E-06	UP
NONMMUT144862.1	-3.021747289	0.000339	DOWN	2.825872	0.000763	UP
NONMMUT152140.1	-3.390813528	0.005418	DOWN	3.671173	0.000159	UP
NONMMUT145717.1	-3.429960838	0.003878	DOWN	4.82329	1.67E-05	UP
ENSMUST00000181045	-3.5774189	2.18E-05	DOWN	4.111429	1.20E-07	UP
MSTRG.8668.1	-3.650059914	8.30E-13	DOWN	2.418835	0.0002	UP
NONMMUT145909.1	-4.44549442	6.50E-05	DOWN	3.575655	3.04E-05	UP
NONMMUT008421.2	-4.495334741	0.000753	DOWN	5.182219	4.44E-06	UP
ENSMUST00000161890	-5.096061065	0.013794	DOWN	6.206952	7.53E-05	UP
NONMMUT128951.1	-5.845021433	2.88E-07	DOWN	4.876355	2.89E-05	UP
NONMMUT065156.2	-7.177240343	5.91E-41	DOWN	6.653339	2.22E-10	UP
NONMMUT026869.2	-8.335434963	1.59E-11	DOWN	7.485915	1.33E-06	UP

The table lists the top 30 of the results for lncRNAs with an up-or downregulation in expression in three groups.

Table 3
Top 30 significantly differential expression mRNAs in mice.

gene name	log2FC (HFDvs CON)	Pvalue (HFDvsCON)	Updown (HFDvs CON)	log2FC (HFD + RSVvs HFD)	Pvalue (HFD + RSVvs HFD)	Updown (HFD + RSVvsHFD)
Gm49388	6.06138	1.92E-10	UP	-2.53021	0.044372	DOWN
Gm26876	3.811306	7.03E-09	UP	-3.11381	5.15E-07	DOWN
4930512H18Rik	3.787461	3.47E-18	UP	-1.20868	0.003987	DOWN
Gm29676	3.283294	0.00530139	UP	-3.86133	0.002862	DOWN
Map6d1	3.074208	0.007729399	UP	-1.72651	0.047048	DOWN
Ppm1n	3.000682	2.93E-08	UP	-1.05825	0.012598	DOWN
Sh3gl2	2.803522	1.83E-09	UP	-2.08107	5.64E-06	DOWN
Clca4a	2.729295	0.000758257	UP	-2.14669	0.002907	DOWN
Gm49347	2.69398	0.016676861	UP	-2.79388	0.016914	DOWN
Gm33543	2.661545	2.23E-13	UP	-1.30568	0.029604	DOWN
Ccl12	2.641596	0.005800303	UP	-3.96508	0.00141	DOWN
Gm9402	2.633552	0.044305865	UP	-2.95627	0.046539	DOWN
Gm48719	2.618363	1.87E-05	UP	-1.43542	0.008835	DOWN
Rpl21-ps12	2.537707	0.000902295	UP	-1.83961	0.012602	DOWN
Gm15478	2.466703	1.04E-05	UP	-1.16718	0.029683	DOWN
Kcnh7	2.453351	3.86E-11	UP	-1.11192	0.016375	DOWN
Socs1	2.44948	4.05E-07	UP	-2.36143	1.61E-06	DOWN
Gm47603	2.39615	2.51E-05	UP	-1.36179	0.007302	DOWN
C130026L21Rik	2.31491	0.023709939	UP	-2.52323	0.024031	DOWN
AY036118	2.26368	0.014427254	UP	-2.08364	0.022577	DOWN
Cish	2.1587	1.43E-14	UP	-2.48736	1.64E-20	DOWN
Cd209e	2.146486	0.001095503	UP	-1.52077	0.033734	DOWN
Dkk3	2.060882	1.16E-07	UP	-1.51887	0.000588	DOWN
Pou2f3	2.046599	0.032113693	UP	-2.67227	0.010465	DOWN
Pcsk1	1.960889	6.87E-07	UP	-1.14143	0.001394	DOWN
Gm26635	1.857674	0.020348988	UP	-1.53523	0.040218	DOWN
B230312C02Rik	1.846494	1.97E-10	UP	-1.85503	2.38E-10	DOWN
4932438H23Rik	1.740581	0.019356615	UP	-1.8725	0.019401	DOWN
Ccl7	1.669165	0.006830603	UP	-1.92417	0.005174	DOWN
Megf11	1.597213	0.002069216	UP	-1.26422	0.028085	DOWN
Sox10	-1.00199	0.00499603	DOWN	1.277467	0.008898	UP
Gm17971	-1.01911	0.001132241	DOWN	1.082473	0.012236	UP
Mgat3	-1.02613	0.002140658	DOWN	1.038285	0.007315	UP
Gas2l3	-1.02807	0.020453198	DOWN	1.139046	0.006303	UP
Bcas1	-1.04182	0.015404068	DOWN	1.7179	0.002295	UP

The table lists the top 30 of the results for mRNA with an up-or downregulation in expression in three groups.

gene name	log2FC (HFDvs CON)	Pvalue (HFDvsCON)	Updown (HFDvs CON)	log2FC (HFD + RSVvs HFD)	Pvalue (HFD + RSVvs HFD)	Updown (HFD + RSVvsHFD)
Asphd2	-1.04528	0.020154215	DOWN	1.010603	0.025998	UP
Gm37537	-1.05529	0.004647624	DOWN	1.013631	0.014094	UP
Fos	-1.07258	0.000205959	DOWN	1.126982	0.002405	UP
Gldn	-1.07534	0.029747688	DOWN	1.119705	0.011748	UP
Pmp22	-1.10369	0.0243704	DOWN	1.272211	0.007779	UP
Sptbn5	-1.10708	0.002406818	DOWN	1.274	0.003898	UP
Plekha4	-1.11677	0.003070017	DOWN	1.306669	0.002928	UP
Kcna6	-1.11915	0.010919737	DOWN	1.15063	0.011805	UP
Gabrr1	-1.12133	0.007296347	DOWN	1.004214	0.027277	UP
Mir1904	-1.12175	0.004769582	DOWN	1.111331	0.011967	UP
Kif19a	-1.14672	0.006248502	DOWN	1.502258	0.001265	UP
Fosl2	-1.16247	1.85E-08	DOWN	1.02334	4.21E-05	UP
Lrrc71	-1.16508	0.023094219	DOWN	1.001178	0.048202	UP
Fhl4	-1.1723	0.034470511	DOWN	1.121767	0.045133	UP
Fa2h	-1.18303	0.034450796	DOWN	1.299243	0.029667	UP
Gm37510	-1.19184	0.004453269	DOWN	1.03012	0.008302	UP
Ppia	-1.19672	0.001831193	DOWN	1.119291	2.62E-05	UP
Tnfsf13b	-1.20579	0.016517031	DOWN	1.142204	0.010129	UP
Tox	-1.21833	0.015176461	DOWN	1.414292	0.001254	UP
Rasgef1c	-1.2224	0.036363327	DOWN	1.405989	0.013403	UP
Mt3	-1.22738	0.007211092	DOWN	1.291177	0.005362	UP
Elovl7	-1.24473	0.016851444	DOWN	1.412536	0.009919	UP
Wnt2b	-1.26686	0.007582771	DOWN	1.527884	0.008061	UP
Tenm2	-1.27034	0.005050296	DOWN	1.05799	0.010664	UP
Mmp27	-1.27782	0.027735632	DOWN	1.191382	0.04508	UP

The table lists the top 30 of the results for mRNA with an up-or downregulation in expression in three groups.

3.5. Cluster analysis results and heat maps of lncRNAs and mRNAs

Through further cluster analysis of differential expression genes, data uncovered that there were significant differences in the expression patterns of lncRNAs and mRNAs among the three groups. Meanwhile, the cluster analysis results of the three groups of lncRNAs were similar to the mRNAs, suggesting that there was a close relationship between the expression of lncRNAs and mRNAs. (Fig. 4A,4B). Venn diagrams indicated that the HFD group had 3276 differentially expressed lncRNAs and 2118 differentially expressed mRNAs compared with the CON group. At the same time, the HFD + RSV group had 1640 differentially expressed lncRNAs and 604 differentially expressed mRNAs in comparison with the HFD group. (Fig. 4C, 4D)

3.6. Functional enrichment analysis of differentially expressed genes

The functions of these different mRNAs were studied by enrichment analysis. GO analysis classified differentially expressed mRNAs into three types: biological process (BP), molecular function (MF), and cellular component (CC). mRNA differential expression mainly took part in the following biological processes: transmembrane receptor protein tyrosine kinase signal transduction, secretion, hormone receptor, cytokine receptor, negative regulation of cell metabolism process, growth, receptor protease-related signaling pathway, cell response to hormone stimulation, and cell response to cytokine stimulation (Fig. 5A). KEGG analysis showed that the differential expression mRNAs involved in ubiquitin-mediated proteolysis, splice, endoplasmic reticulum stress protein, prolactin signaling pathway, MAPK signaling pathway, PI3K-Akt signaling pathway, osteoclast differentiation, microRNA in cancer, JAK-STAT signaling pathway, insulin signaling pathway, and estrogen signaling pathway (Fig. 5B). SOCS1 plays a vital role in the insulin signaling pathway, which was reported to involve in the development of IR.

3.7. RT-qPCR validation in vivo

To confirm the validity of the sequencing results, we next randomly picked 4 differential lncRNAs, two lncRNAs up-regulated in HFD, down-regulation of HFD + RSV (NONMMUT044897.2, NONMMUT005295.2), and two lncRNAs with a reverse trend (NONMMUT128951.1, NONMMUT145909.1). Selected lncRNAs expression levels were consistent with the sequencing results (Fig. 6A-D), but there was no statistical difference in the increase of NONMMUT128951.1 in the HFD + RSV group. Among the verified lncRNAs, NONMMUT044897.2 has a higher expression level. In addition, GO and KEGG analysis indicated that differential expression mRNAs enriched in the insulin signaling pathway. Hence, we chose this pathway and predicted the closely related mRNA SOCS1 and NONMMUT044897.2 through pathway analysis, and the trends of the two were consistent. To elucidate the interaction between them, we constructed a related lncRNA-miRNA-mRNA network diagram. The results revealed that this lncRNA regulates mRNA SOCS1 through miR-7051-5p and miR-762 (Fig. 6F). To further explore its potential molecular mechanism, we applied NonCode and miRBase database analysis and found that there was base pairing in the sequence of NONMMUT044897.2 and the sequence of miR-7051-5p. At the same time, according to the prediction results of Targetscan, it can be found that SOCS1 is a miR-7051-5p target (Fig. 6G). According to the above results, NONMMUT044897.2 may regulate SOCS1 through miR-7051-5p. Therefore, this study further verified the expression of miR-7051-5p mRNA through RT-qPCR (Fig. 6E), miR-7051-5p mRNA was down-regulated in HFD and up-regulated in HFD + RSV.

3.8. Establishment of a cell model of PA-induced IR

The cells were transferred to medium with and without 0.25mM PA, and glucose concentrations were determined at 0 h, 8 h, 16 h, and 24 h. There was no significant difference in CON and PA group at 0 h, 8 h, and 16h, however, the glucose concentration of the PA group was drastically elevated at 24 h in comparison with the CON group, indicating that the IR model was successfully established (Fig. 7A). Besides, the glucose concentration was dramatically relieved at 24 h when RSV treatment (Fig. 7B).

The cell survival rate of C2C12 cells 24 hours after RSV of 30 ~ 100 μm was observed. The results showed that RSV of 30μm had no significant influence on the survival rate of C2C12 cells (Fig. 7C). The cell survival rate of the PA group (84%) was lower than that of the Con group (89.6%), and the PA + RSV 30 μM group (85%) was higher than that of the PA group. However, there was no statistical difference among the three groups (Fig. 7D).

3.9. RT-qPCR validation in vitro

Two lncRNAs up-regulated in PA, downregulation of PA + RSV (NONMMUT044897.2, NONMMUT139818.1) and three lncRNAs with reverse trend (NONMMUT071570.2、NONMMUT065156.2、NONMMUT00000181045). The expression levels of selected lncRNAs were consistent with the sequencing results (Fig. 8A-E), but there was no statistical difference in the increase of NONMMUT00000181045 in the PA + RSV group. To verify the relationship between NONMMUT044897.2 and RSV in vitro, lentivirus transfected C2C12 cells. Results shown that as compared with the CON group, NONMMUT044897.2 expression was robustly increased in the PA group and PA + shRNA-NC group. The PA + shRNA-NONMMUT044897.2 group suppressed the expression of NONMMUT044897.2 when compared to the PA group. RSV administration also decreased the expression of NONMMUT044897.2 in comparison with the PA group (Fig. 8G).

Relative to the CON group, the miR-7051-5p mRNA in the PA group and the PA + shRNA-NC group was significantly declined, while knockdown of NONMMUT044897.2 and RSV treatment prominently enhanced miR-7051-5p mRNA level (Fig. 8F).The concentration of glucose in the medium of the PA group and the PA + shRNA-NC group was substantially increased when compared with the CON group. NONMMUT044897.2 silence and RSV treatment strikingly overturned the glucose concentrations in the medium (Fig. 8H). Knockdown of NONMMUT044897.2 distinctively upregulated the p-AKT, p-GSK3β, and GLUT4 protein levels, and greatly reduced the SOCS1 protein level, when compared with the PA group. RSV treatment had a similar effect on p-AKT, p-GSK3β, GLUT4, and SOCS1 protein levels which were comparable to the NONMMUT044897.2 silence (Fig. 8I-N).

4. Discussion

Resveratrol is used in the field of insulin resistance improvement [22, 23]. RSV increases the expression of microencapsulated protein 3 (CAV-3), thereby allowing skeletal muscle cells to carry glucose the protein GLUT4 activates the transfer from the cytoplasm to the cell membrane, which in turn increases the ability of myocytes to transport glucose and improve insulin resistance[24]. In addition, RSV promotes the beta-oxidation process of fatty acids in the cell mitochondria [25], so that intracellular lipids are better metabolized. RSV also improves IR in skeletal muscle by reducing SNARE proteins in diabetic rats[26],which is involved in GLUT4 transport. Meanwhile, RSV attenuates insulin-stimulated AKT phosphorylation by eliminating insulin-induced ROS production in skeletal muscle [27].

A large amount of experiments has verified the therapeutic effect of RSV in IR. In this study, we demonstrated that the influence of RSV in the improvement of insulin resistance in high-fat diet mice as reported previously [24, 25, 26, 27]. Not only did blood glucose, insulin index, and area under the curve (AUC) decreased in high-fat mice after applying RSV, but also improved blood lipid levels. RSV treatment improved high-fat diet-induced mice insulin resistance by restoring insulin signaling pathway gene expression. After the intervention of RSV, the mRNA and protein expression levels of p-AKT, p-GSK3β and GLUT4 increased significantly after RSV application.

The expression of lncRNA has spatiotemporal specificity, and it participates in the process of gene regulation and biological function regulation in epigenetics, transcription, and post-transcription levels [28]. Abnormal expression of lncRNAs could affect the occurrence and development of human diseases, including non-alcoholic fatty liver, various cancers, and T2DM [29]. At present, the function of most lncRNAs is completely unknown. Previous studies[30, 31] by our group have demonstrated that RSV can improve hepatic IR by regulating lncRNA NONMMUT058999.2 and NONMMUT008655.2 in IR models .Whether RSV could improve IR by regulating the expression of lncRNAs in skeletal muscle remains undefined. In this study, we further studied skeletal muscle, a different tissue than previous studies, and found a novel lncRNA NONMMUT044897.2 that may be involved in resveratrol's improvement of skeletal muscle IR in vivo.

High-throughput sequencing showed that there were 3276 differential lncRNAs and 2118 mRNAs in HFD mice compared to the CON group, and 1640 differential lncRNAs and 604 mRNAs compared to the HFD + RSV group. We further provided 338 mRNAs and 629 lncRNAs whose expression was reversed between HFD and HFD + RSV groups, suggesting that RSV is under a strong role in the overall alteration of skeletal muscle gene expression. Moreover, via RT-qPCR uncovered that RSV improved IR by regulating the expression of lncRNAs in skeletal muscle. As mentioned above, the verified lncRNAs were consistent with the sequencing results and NONMMUT044897.2 was highly expressed. GO and KEGG analysis uncovered that the differential genes were part of the insulin signaling pathway. We found that NONMMUT044897.2 was associated with SOCS1, which is critically involved in the insulin signaling pathway, so we selected this lncRNA for further study, which hadn't been reported before.

SOCS1 is a specific negative regulator that regulates the JAK/STAT pathway [32]. The expression of SOCS1 increases under insulin resistance and overexpression of SOCS1 decreases the phosphorylation of IRS-1; overexpression of SOCS-1 can inhibit insulin-induced glycogen synthesis in L6 myotubes [33]. AKT has essential roles in many signaling pathways, such as cell survival and cell metabolism. AKT is the center of the insulin signaling pathway, which regulates glucose and lipid metabolism. Activated AKT can stimulate the translocation of insulin-sensitive GLUT4 to the cell membrane through its downstream substrate ASl60 to increase glucose uptake; it can also phosphorylate GSK3β to inhibit its activity, promote glycogen synthesis, lower blood sugar, and improve IR [34]. A high fat diet can result in the decrease of skeletal muscle IRS-1, P13K, AKT, GLUT4 gene expression, reduce p-AKT (ser473), p- GSK3β protein expression. Studies have reported that overexpression of SOCS1 can inhibit the phosphorylation and activation of IRS-1[32, 33], which in turn inhibits the activation of AKT, indicating that there is an important link between AKT and SOCS1. We found that in IR model mice, mRNA and protein expression levels of SOCS1 was significantly increased, RSV treatment reversed this trend, thereby improving insulin resistance and decreasing blood glucose.

Numerous studies have demonstrated that lncRNAs may involve in human diseases by regulating miRNA expression [35, 36]. The co-expression network diagram uncovered the possible regulatory roles of candidate lncRNA NONMMUT044897.2 could regulate SOCS1 through two different miRNAs. To further clarify the relationship between NONMMUT044897.2 and SOCS1, we constructed NONMMUT044897.2 and miR-7051-5p, miR-7051-5p and SOCS1base pairing maps based on the NonCode and miRBase databases and the Targetscan database. These results indicated that NONMMUT044897.2 might regulate the expression of SOCS1 through miR-7051-5p. Future studies may perform luciferase assays to verify the interactions between NONMMUT044897.2, miR-7051-5p, and SOCS1.

We confirmed that knockdown of NONMMUT044897.2 increased miR-7051-5p levels, promoted gene expression of insulin signaling (p-AKT, p-GSK3β, GLUT4). Meanwhile, the expression of SOCS1 was suppressed by silencing NONMMUT044897.2. Moreover, knockdown of NONMMUT044897.2 led to reduced glucose concentration, similar to the phenotypes induced by RSV treatment, indicating that resveratrol improves skeletal muscle insulin resistance through downregulating the lncRNA NONMMUT044897.2.

5. Conclusion

This research profiled the differential expression of lncRNAs between the IR mice model and RSV treatment and further revealed the potential regulated lncRNA NONMMUT044897.2. Much more work remains to be done to prove the relationship between the NONMMUT044897.2/miR-

7051-5p/SOCS1and RSV in the IR model. There are also limitations. First, in vivo animal models are also needed to further perform by silencing NONMMUT044897.2 to verify the influence on insulin resistance. Second, overexpression of NONMMUT044897.2 should be done in vitro. Third, knockdown of the NONMMUT044897.2 in the RSV group should be done to observe the influence on the insulin resistance model. Overall, our data indicated that RSV could promote skeletal muscle insulin resistance, at least partially, via a lncRNA NONMMUT044897.2 /miR-7051-5p/SOCS1 pathway, thereby provides a new perspective for RSV treatment of IR in skeletal muscle.

Declarations

Ethics approval and consent to participate

All animal experiments were performed with approval from the Institutional Animal Care and Use Committee of Hebei General Hospital, Hospital.

Consent for publication

N/A.

Availability of data and materials

All data, analytic methods, and study materials presented within this article are available for other investigators from the corresponding authors on reasonable request.

Competing interests

The authors declare that they have no conflicts of interest to this work.

Funding

This study was supported by the grant from the Natural Science Foundation of Hebei Province (No. H201830-7071).

Authors' contributions

Conceptualization and design of the study: Guangyao Song. Drafting the manuscript: Zhihong Liu. Analysis of data: Zhihong Liu, Zhimei Zhang, Chao Wang, Xing Wang, Hanying Xing. Validation: Zhimei Zhang, Chao Wang, Xing Wang, Hanying Xing. Revising the manuscript critically for important intellectual content: Guangyao Song. Approval of the version of the manuscript to be published: Guangyao Song, Zhihong Liu, Zhimei Zhang, Chao Wang, Xing Wang, Hanying Xing.

Acknowledgements

We sincerely thank the teachers at the Clinical Medical Research Centre of Hebei General Hospital who helped us during the experiment.

Abbreviations

lncRNA, long non-coding RNA; IR, insulin resistance; RSV, resveratrol; HFD, high-fat diet; SOCS1,Suppressor of Cytokine Signaling 1; IPGTT, intraperitoneal glucose tolerance test; AUC, area under the curve; TC, total cholesterol; TG, triglyceride; HDL-C, high-density lipoprotein cholesterol; LDL-C, low-density lipoprotein cholesterol; FFA, free fatty acid; GO, Gene Ontology; KEGG, Kyoto Encyclopedia of Genes and Genomes; DMEM, Dulbecco's modified Eagle's medium; PA, palmitate; QUICKI, quantitative insulin sensitivity index.

References

1. Czech MP. Insulin action and resistance in obesity and type 2 diabetes. Nat Med. 2017;23:804–14.
2. Merz KE, Thurmond DC. Role of Skeletal Muscle in Insulin Resistance and Glucose Uptake. Compr Physiol. 2020;10:785–809.
3. Palsamy P, Subramanian S. Resveratrol, a natural phytoalexin, normalizes hyperglycemia in streptozotocin-nicotinamide induced experimental diabetic rats. Biomed Pharmacother. 2008;62:598–605.
4. Gómez-Zorita S, González-Arceo M, Trepiana J, Aguirre L, Crujeiras AB, Irles E, Segues N, Bujanda L, Portillo MP. Comparative Effects of Pterostilbene and Its Parent Compound Resveratrol on Oxidative Stress and Inflammation in Steatohepatitis Induced by High-Fat High-Fructose Feeding. Antioxidants (Basel). 2020;9:1042.
5. Singh AP, Singh R, Verma SS, Rai V, Kaschula CH, Maiti P. S.C.Gupta, Health benefits of resveratrol: Evidence from clinical studies. Med Res Rev. 2019;39:1851–91.

6. Carpéné C, Les F, Cásedas G, Peiro C, Fontaine J, Chaplin A, Mercader J, López V. Resveratrol Anti-Obesity Effects: Rapid Inhibition of Adipocyte Glucose Utilization, Antioxidants (Basel) 8(2019) 74.
7. Luo G, Huang BQ, Qiu X, Xiao L, Wang N, Gao Q, Yang W. L.P.Hao, Resveratrol attenuates excessive ethanol exposure induced insulin resistance in rats via improving NAD^+ /NADH ratio, Mol Nutr Food Res 61(2017).
8. Den Hartogh DJ, Vlavcheski F, Giacca A, Tsiani E. Attenuation of Free Fatty Acid (FFA)-Induced Skeletal Muscle Cell Insulin Resistance by Resveratrol is Linked to Activation of AMPK and Inhibition of mTOR and p70 S6K. Int J Mol Sci. 2020;21:4900.
9. Vlavcheski F, Den Hartogh DJ, Giacca A. E. Tsianiet al, Amelioration of High-Insulin-Induced Skeletal Muscle Cell Insulin Resistance by Resveratrol Is Linked to Activation of AMPK and Restoration of GLUT4 Translocation, Nutrients12(2020):914.
10. Zhang YJ, Zhao H, Dong L, Zhen YF, Xing HY, Ma HJ, Song GY. Resveratrol ameliorates high-fat diet-induced insulin resistance and fatty acid oxidation via ATM-AMPK axis in skeletal muscle. Eur Rev Med Pharmacol Sci. 2019;23:9117–25.
11. Quinn JJ, Chang HY. Unique features of long non-coding RNA biogenesis and function. Nat Rev Genet. 2016;17:47–62.
12. Constanty F, Shkumatava A. lncRNAs in development and differentiation: from sequence motifs to functional characterization, Development 148 (2021).
13. Thapar R, Wang JL, Hammel M, Ye RQ, Liang K, Sun CC, Hnizda A, Liang SK, Maw SS, Lee L, Villarreal H, Forrester I, Fang SJ, Tsai M, Blundell TL, Davis AJ, Lin C, Lees-Miller SP, Strick TR, Tainer JA. Mechanism of efficient double-strand break repair by a long non-coding RNA. Nucleic Acids Res. 2020;48:10953–72.
14. Cho H, Li YB, Archacki S, Wang F, Yu G, Chakrabarti S, Guo Y, Chen QY, Wang QK. Splice variants of lncRNA RNA ANRIL exert opposing effects on endothelial cell activities associated with coronary artery disease. RNA Biol. 2020;17:1391–401.
15. Feng YC, Liu XY, Teng L, Ji Q, Wu YY, Li JM, Gao W, Zhang YY, La T, Tabatabaee H, Yan XG, Jamaluddin MB, Zhang DD, Guo ST, Scott RJ, Liu T, Thorne RF, Zhang XD. L. Jin ,c-Myc inactivation of p53 through the pan-cancer lncRNA MILIP drives cancer pathogenesis. Nat Commun. 2020;11(1):4980.
16. Liu SX, Zheng F, Xie KL, Xie MR, Jiang LJ. Y.Cai, Exercise Reduces Insulin Resistance in Type 2 Diabetes Mellitus via Mediating the lncRNA MALAT1/MicroRNA-382-3p/Resistin Axis. Mol Ther Nucleic Acids. 2019;18:34–44.
17. Chen DL, Shen DY, Han CK, Tian Y. LncRNA MEG3 aggravates palmitate-induced insulin resistance by regulating miR-185-5p/Egr2 axis in hepatic cells. Eur Rev Med Pharmacol Sci. 2019;23:5456–67.
18. Wang YG, Hu YN, Sun CX, Zhuo S, He ZS, Wang H, Yan MH, Liu J, Luan Y, Dai CG, Yang YG, Huang R, Zhou B, Zhang F, Zhai QW. Down-regulation of Risa improves insulin sensitivity by enhancing autophagy. FASEB J. 2016;30:3133–45.
19. Shen X, Zhang YJ, Zhang X, Yao YW, Zheng YJ, Cui XW, Liu C, Wang Q, Li JZ. Long non-coding RNA Bhmt-AS attenuates hepatic gluconeogenesis via modulation of Bhmt expression. Biochem Biophys Res. 2019;Commun516:215–21.
20. Livak KJ, Schmittgen TD. Analysis of relative gene expression data using real-time quantitative PCR and the 2(-delta C(T)) method. Methods. 2001;25:402–8.
21. Liu M, Qin J, Hao YR, Liu M, Luo J, Luo T. L.Wei, Astragalus polysaccharide suppresses skeletal muscle myostatin expression in diabetes: involvement of ROS-ERK and NF-kB Pathways, Oxid Med Cell Longev2013(2013)782497.
22. Oshaghi EA, Goodarzi MT, Higgins V, Adeli K. Role of resveratrol in the management of insulin resistance and related conditions: Mechanism of action,Crit. Rev Clin Lab Sci. 2017;54:267–93.
23. Sadeghi A, Seyyed Ebrahimi SS, Golestani A, Meshkani R. Resveratrol Ameliorates Palmitate-Induced Inflammation in Skeletal Muscle Cells by Attenuating Oxidative Stress and JNK/NF-κB Pathway in a SIRT1-Independent Mechanism. J Cell Biochem. 2017;118:2654–63.
24. Tana Z, Zhoua LJ, Mu PW, Liu SP, Chen SJ, Fu XD. T.H.Wang,Caveolin-3 is involved in the protection of resveratrol against high-fat-diet-induced insulin resistance by promoting GLUT4 translocation to the plasma membrane in skeletal muscle of ovariectomized rats. J Nutr Biochem. 2012;23:1716–24.
25. Chen LL, Zhang HH, Zheng J, Hu X, Kong W, Wang DHu,SX, Zhang P. Resveratrol attenuates high-fat diet–induced insulin resistance by influencing skeletal muscle lipid transport and subsarcolemmal mitochondrial β-oxidation. Metabolism. 2011;60:1598–609.
26. Farimani ARezaei, Goodarzi MT, Saidijam M, Yadegarazari R, Zarei S, Asadi S. Effect of resveratrol on SNARE proteins expression and insulin resistance in skeletal muscle of diabetic rats. Iran J Basic Med Sci. 2019;22:1408–14.
27. Quana YY, Hua SN, Li W, Zhan MX, Li Y, Lu LG. Resveratrol bidirectionally regulates insulin effects in skeletal muscle through alternation of intracellular redox homeostasis. Life Sci. 2020;242:117188.
28. I.Tsagakis K, Douka I, .Birds JL, Aspden. Long non-coding RNAs in development and disease: conservation to mechanisms. JPathol. 2020;250:480–95.
29. Xiong L, Wu LT, Li J, He WM, Zhu XN, Gong YY. H.P. Xiao.LncRNA-Malat1 is involved in lipotoxicity-induced β-cell dysfunction and the therapeutic effect of exendin-4 via Ptbp1, Endocrinology 161(2020) bqaa065.

30. Shu L, Hou G, Zhao H, Huang W, Song G, Ma H. Resveratrol improves high-fat diet-induced insulin resistance in mice by downregulating the lncRNA NONMMUT008655.2. Am J Transl Res. 2020;12:1–18.
31. Shu L, Hou G, Zhao H, Huang W, Song G, Ma H. Long non-coding RNA expression profiling following treatment with resveratrol to improve insulin resistance. Mol Med Rep. 2020;22:1303–16.
32. Lu L, Ye XH, Yao Q, Lu AJ, Zhao Z, Ding Y, Meng CC, Yu WL, Du YF. J.L. Cheng,Egr2 enhances insulin resistance via JAK2/STAT3/SOCS-1 pathway in HepG2 cells treated with palmitate. Gen Comp Endocrinol. 2018;260:25–31.
33. Rui LY, Yuan MS, Frantz D, Shoelson S, White MF. SOCS-1 and SOCS-3 block insulin signaling by ubiquitin-mediated degradation of IRS1 and IRS2. J Biol Chem. 2002;277:42394–8.
34. Huang XJ, Liu GH, Guo J, Su ZQ. The PI3K/AKT pathway in obesity and type 2 diabetes. Int J Biol Sci. 2018;14:1483–96.
35. Cardoso AM, Morais CM, Rebelo O, H Tão, Barbosa M, Pedroso de Lima MC, Jurado AS. Downregulation of long non-protein coding RNA MVIH impairs glioblastoma cell proliferation and invasion through a miR-302a-dependent mechanism. Hum Mol Genet. 2021;12:ddab009.
36. Zheng JH, Tan Q, Chen H, Chen K, Wang HF, Chen ZL, Xi Y, Yin HS 1, Lai K., Y.J. Liu ,lncRNA–SNHG7–003 inhibits the proliferation, migration and invasion of vascular smooth muscle cells by targeting the miR–1306–5p/SIRT7 signaling pathway, Int J Mol Med 16(2020).

Figures

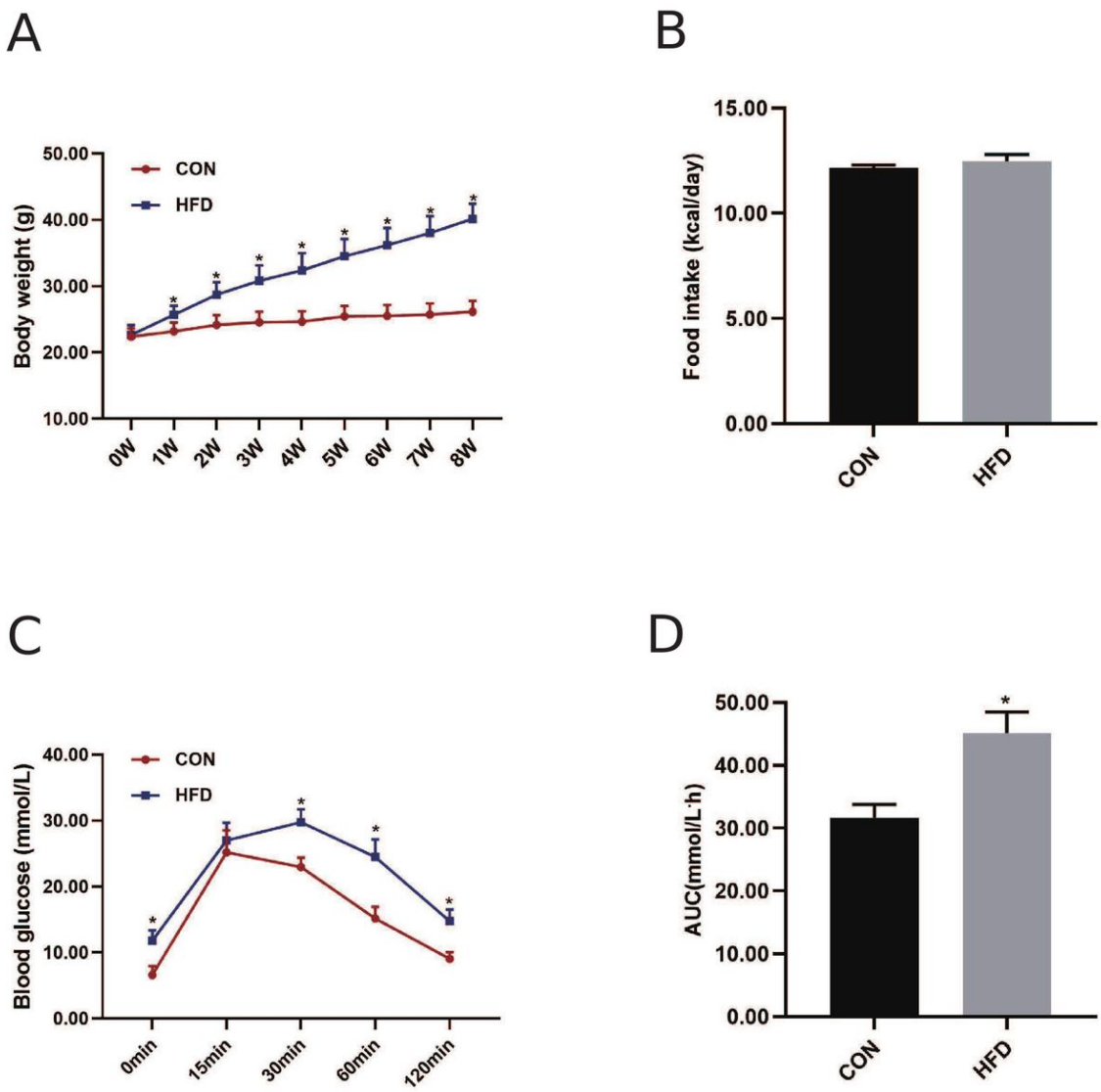

Figure 1

Body weights, food intake, and IPGTT experiments of C57BL/6J mice. A. Body weight; B. Food intake; C. Blood glucose levels of IPGTT; D. The area under the curve for glucose levels. Data are expressed as mean ± SD (n = 14). *P < 0.05 vs CON group.

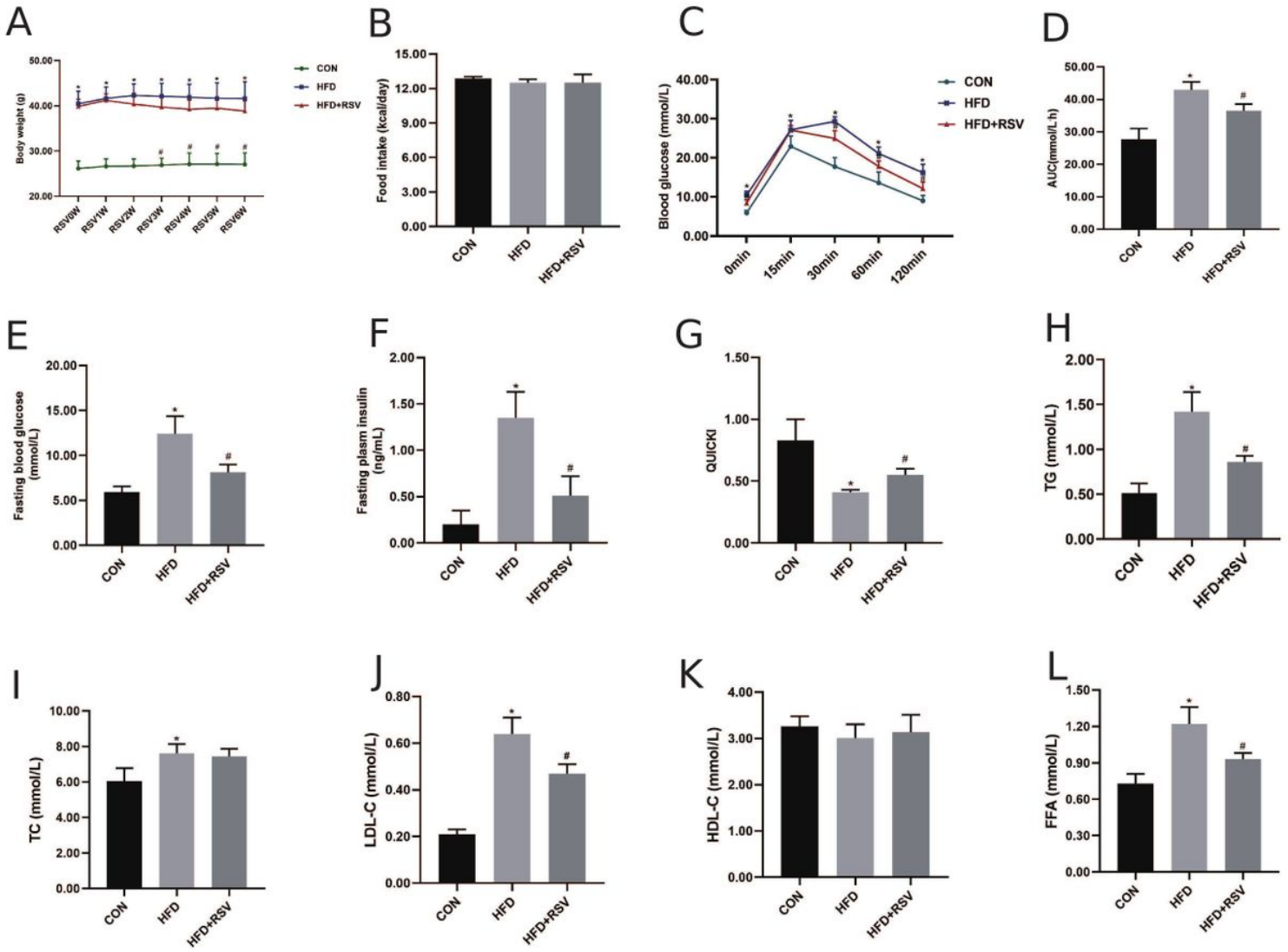

Figure 2

Effects of resveratrol on the body weight、insulin resistance and lipid levels in the mice. A. Body weight; B. Food intake; C. Blood glucose levels after IPGTT; D. The area under the curve for glucose levels; E. Fasting blood glucose; F. Fasting plasma insulin; G. Quantitative insulin sensitivity check index. H. Triglyceride levels; I. Total cholesterol levels; J. Low-density lipoprotein cholesterol levels; K High-density lipoprotein cholesterol levels; L. Free fatty acid levels. Data are expressed as mean ± SD (n = 14). *P < 0.05 vs CON, #P < 0.05 vs HFD.

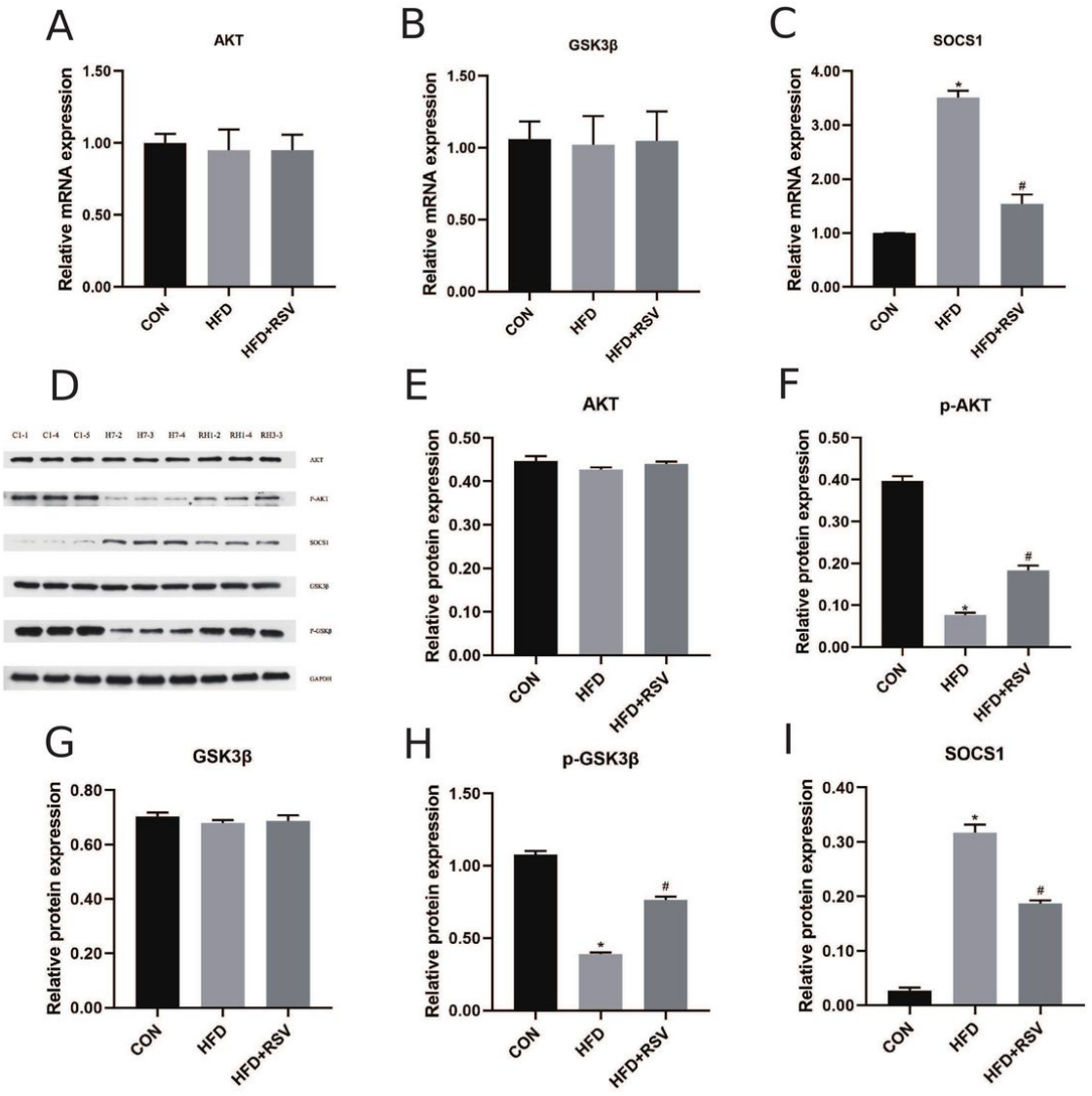

Figure 3

Effects of resveratrol on the insulin signaling pathway in three groups. A. AKT mRNA; B. GSK3β mRNA; C.SOCS1 mRNA; D. Bands of Western blot; Densitometry analysis of AKT (E), p-AKT(F), GSK3β(G), p-GSK3β(H), SOCS1(I). Data are expressed as the mean ± SD (n=3). *P < 0.05 vs CON, #P < 0.05 vs HFD.

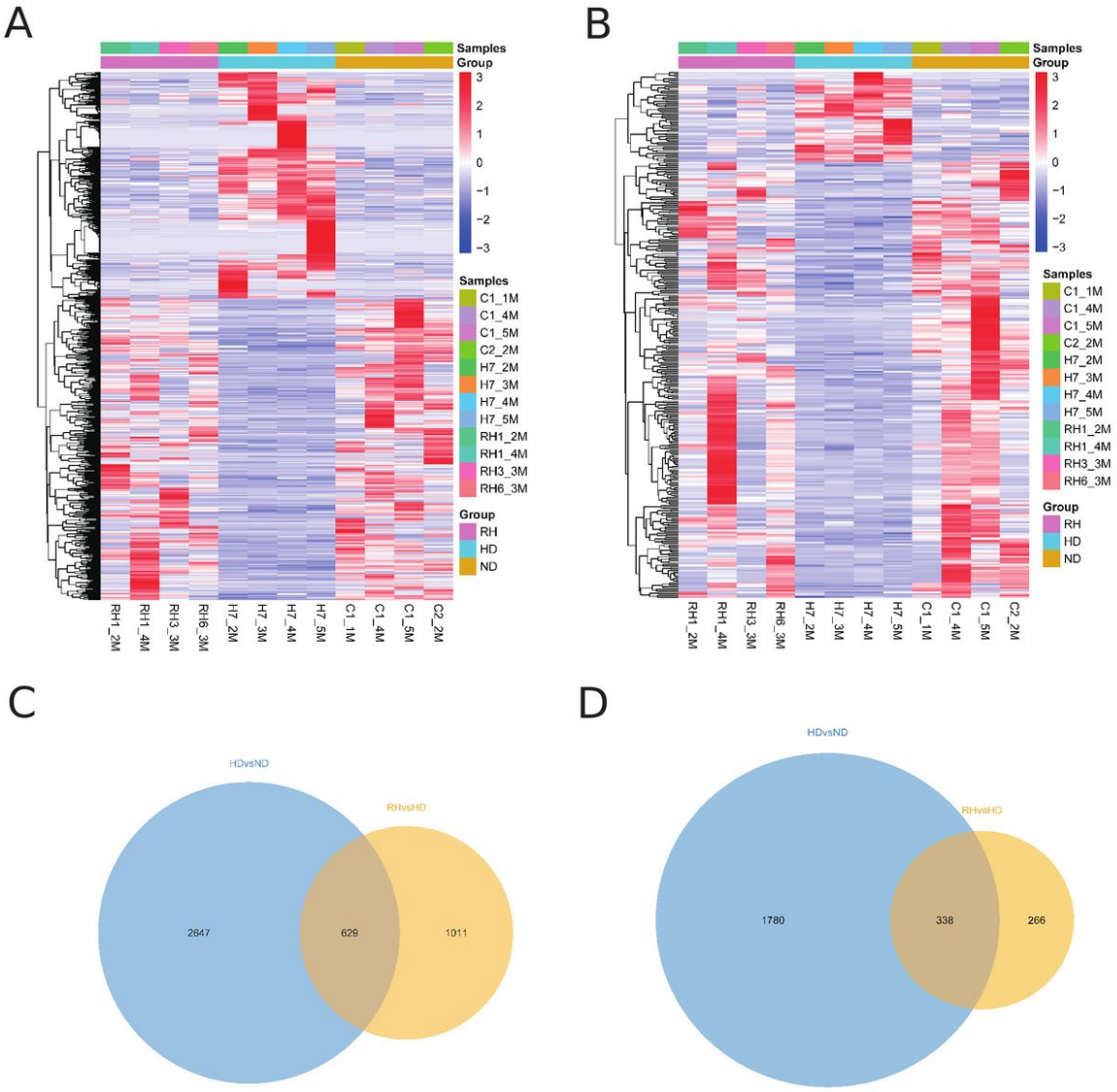

Figure 4

Profiles of differential expression genes in three groups. (A) Hierarchical clustering of lncRNAs and (B)mRNAs. The red area shows up-regulated lncRNAs (or mRNAs).The blue area shows down-regulated lncRNAs (or mRNAs). C. Differential expression lncRNAs Venn diagram in three groups D. Differential expression mRNAs Venn diagram in three groups.

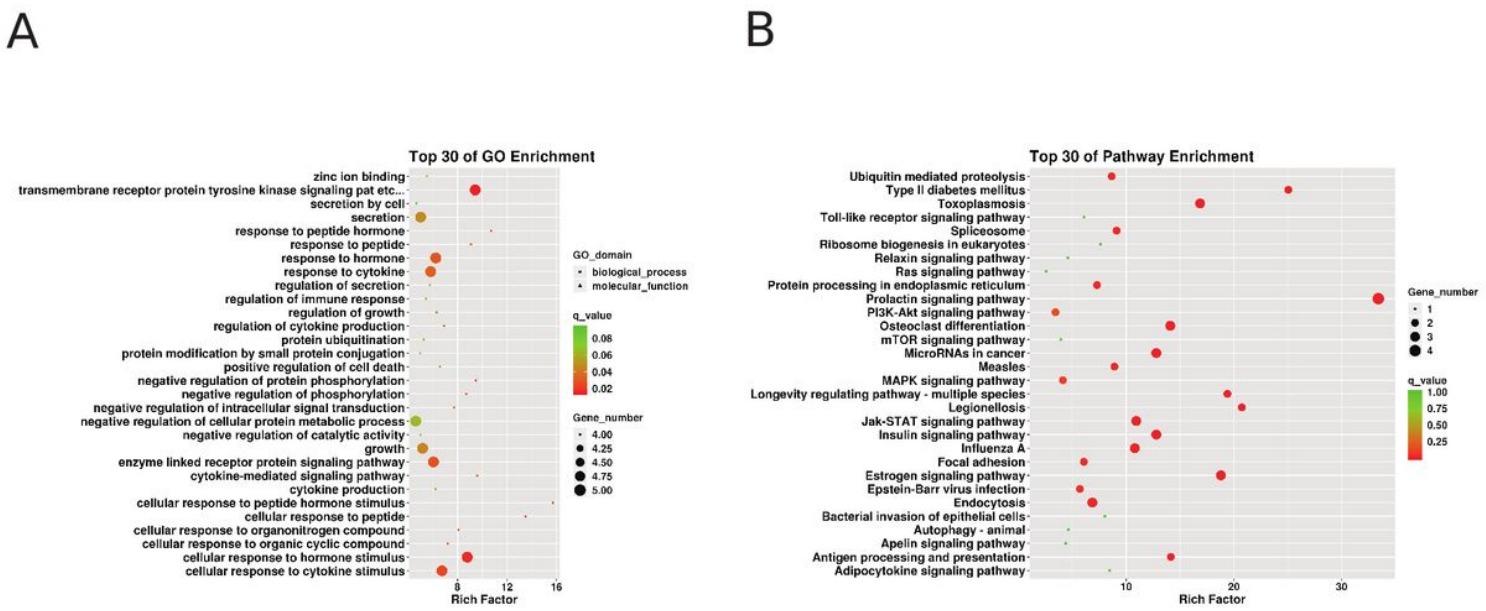

Figure 5

Gene ontology and pathway analysis of differential expression genes in three groups. A. Top 30 GO terms of differential expression mRNAs; B. Top 30 KEGG pathways of differential expression mRNAs.

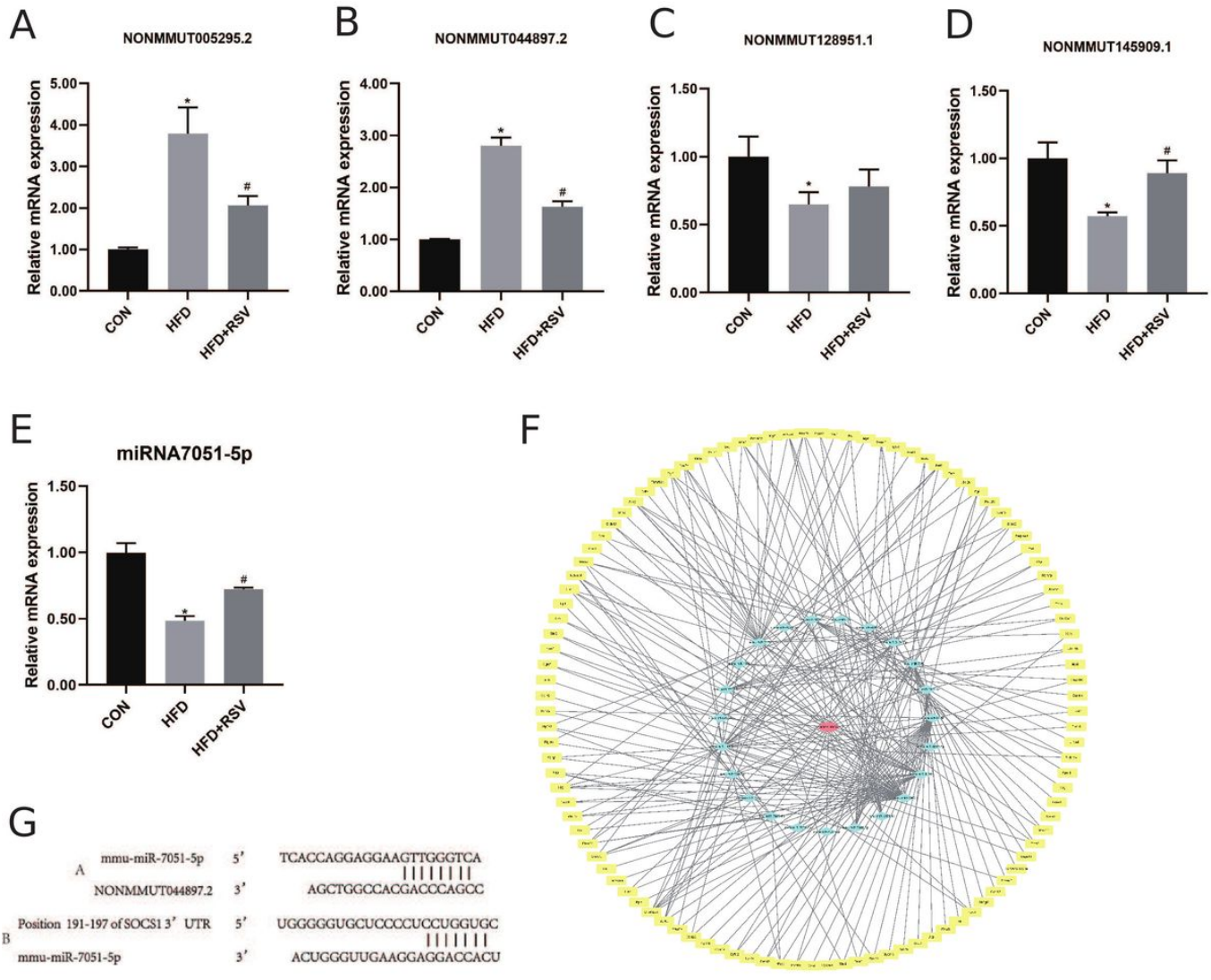

Figure 6

Validation of lncRNAs by RT-qPCR in vivo. A. NONMMUT005295.2; B.NONMMUT044897.2; C.NONMMUT128951.1; D.NONMMUT145909.1. E. miRNA-7051-5p mRNA expression in different groups. F. The NONMMUT044897.2 lncRNA-miRNA-mRNA network. G. The positions of miR-7051-5p binding sites on NONMMUT044897.2 and the positions of miR-7051-5p binding sites on SOCS1 are shown. Data are expressed as the mean ± SD. (n=3).*P < 0.05 vs CON, #P <0.05 vs HFD.

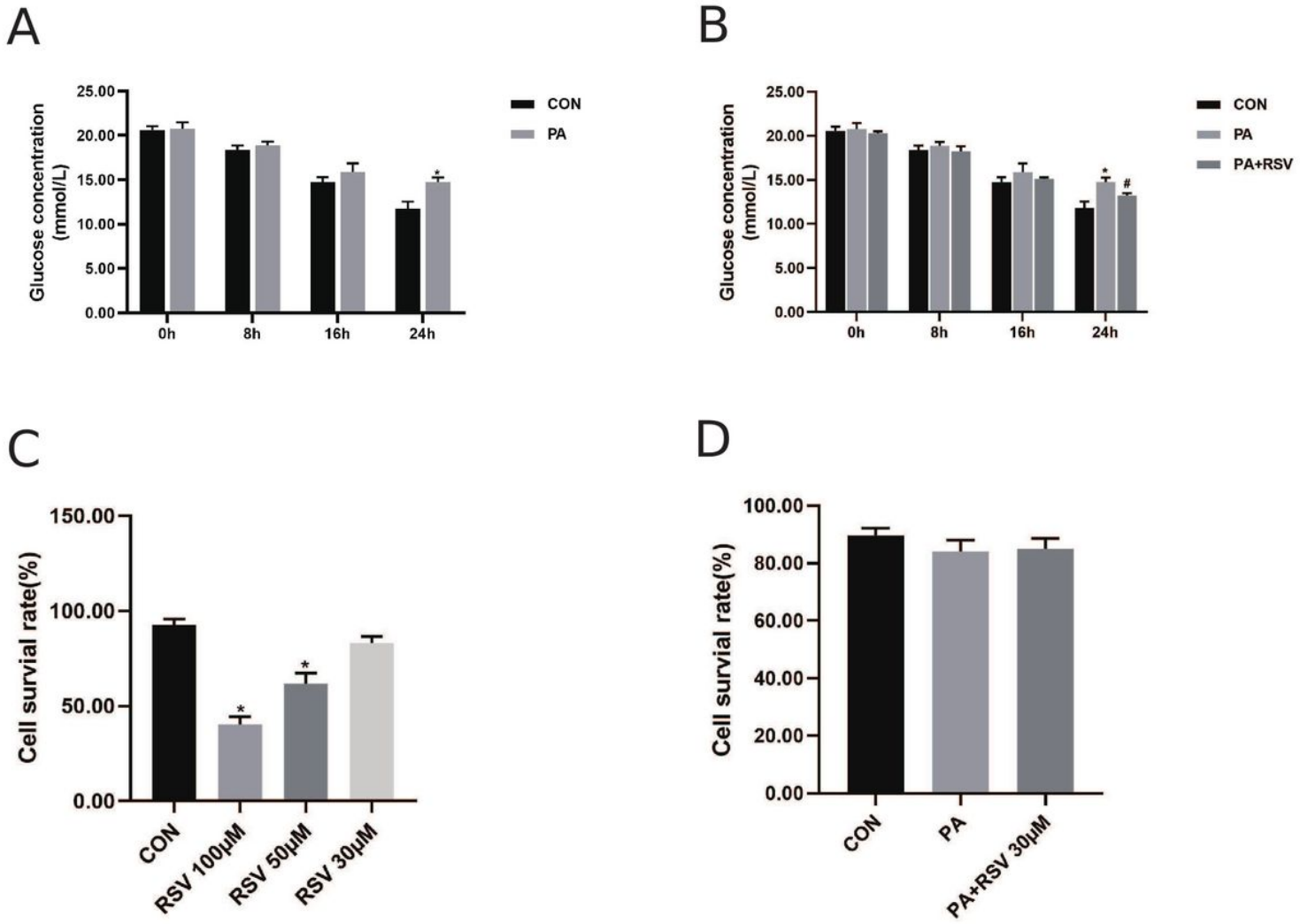

Figure 7

Resveratrol reduced PA-induced glucose concentration in vitro. A. The glucose concentration in the medium after 0, 8, 16, and 24 h treatment with PA; B. The glucose concentration in the medium after 0, 8, 16 and 24 h treatment with PA and RSV; C. Cell survival rate after 24 h treatment with different concentrations of RSV; D. Cell survival rates of the different groups after PA and RSV treatments; Data are shown as the mean ± SD. (n=6).*P < 0.05 vs CON, #P < 0.05 vs PA.

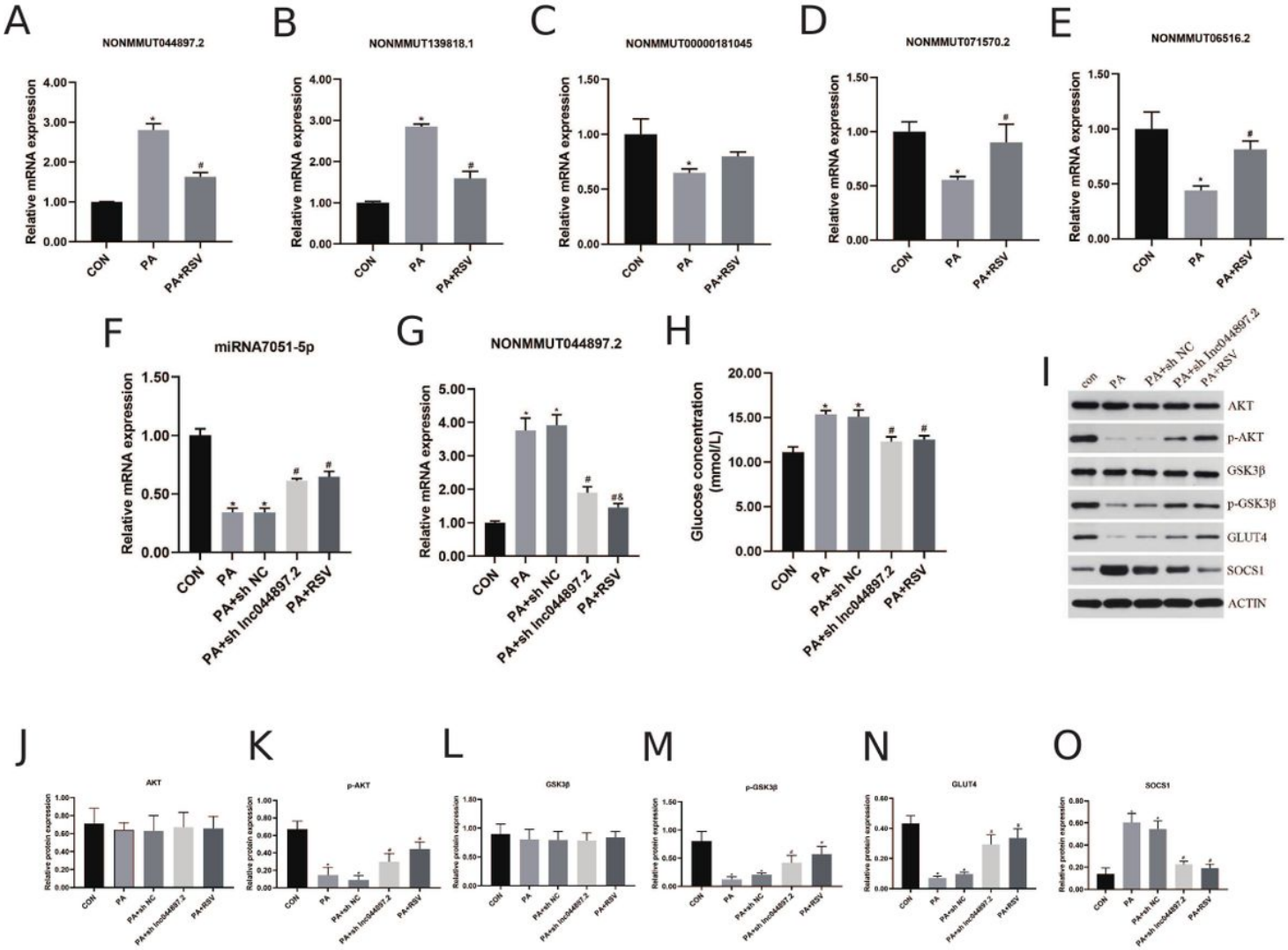

Figure 8

Resveratrol improved skeletal muscle insulin resistance through downregulating the lncRNA NONMUT044897.2 in vitro. A. Validation of lncRNA (NONMMUT044897.2) by RT-qPCR; B. Validation of lncRNA (NONMMUT139818.1) by RT-qPCR; C. Validation of lncRNA (NONMMUT00000181045) by RT-qPCR; D. Validation of lncRNA (NONMMUT071570.2) by RT-qPCR; E. Validation of lncRNA (NONMMUT06516.2) by RT-qPCR; F. The expression of miR-7051-5p mRNA after shRNA transfected into C2C12 cells in different groups; G. The expression of NONMMUT044897.2 mRNA after shRNA transfected into C2C12 cells in different groups; H. Glucose concentrations in the culture medium after shRNA transfected into C2C12 cells in different groups; I. Protein bands of insulin signaling pathway molecules; Densitometry analysis of (J) AKT, (K) p-AKT, (L) GSK3β, (M) p-GSK3β, (N) GLUT4, (O) SOCS1. Data are presented as the mean ± SD. (n=3). *P < 0.05 vs CON, #P < 0.05 vs PA, δP < 0.05 vs PA+shRNA-NONMMUT044897.2.